Ornamental Plant Research

ARTICLE

Open Access

https://doi.org/10.48130/opr-0026-0014

Ornamental Plant Research **2026**, 6: e021

Integrated transcriptomic and metabolomic profiling elucidates the regulation of flavonoid composition and biosynthesis in *Rosa rugosa* hip

Lulu Li[1,2#], Tao Jiang[3#], Shunhao Guo[1,2], Huali Zhu[1,2], Wei Li[1,2], Yizeng Lu[4*] and Cuiping Zhang[1,2*]

[1] *College of Landscape Architecture and Forestry, Qingdao Agricultural University, Qingdao 266100, China*
[2] *Shandong Provincial Key Laboratory of Salt-Alkali Tolerant Grass and Tree Germplasm Innovation, Qingdao 266100, China*
[3] *Jinan Baihe Garden Group Co., Ltd., Jinan 250000, China*
[4] *Shandong Provincial Center of Forest and Grass Germplasm Resources, Jinan 250000, China*
[#] Authors contributed equally: Lulu Li, Tao Jiang
* Correspondence: luyizeng@126.com (Lu Y); zcp116@126.com (Zhang C)

Abstract

Rosa rugosa hips are a valuable resource rich in flavonoids with significant health benefits, though the regulatory mechanisms underlying flavonoid biosynthesis remain unclear. In *R. rugosa* hip, the chlorophyll content decreased significantly during hip ripening from the green (F0) to the yellow (F1) and red (F2) stages. In contrast, total flavonoid content peaked at the F1 stage, while anthocyanin and carotenoid levels showed a concomitant increase. To investigate the regulatory mechanisms, we performed integrated transcriptomic and metabolomic analyses of wild *R. rugosa* hips at the F1 and F2 stages. Transcriptomic data revealed 4,329 DEGs, which were predominantly enriched in 'Metabolic pathways' and 'Biosynthesis of secondary metabolites' by KEGG pathway enrichment analysis. Notably, 62 upregulated DEGs were assigned to specific flavonoid-related biosynthesis pathways. Meanwhile, metabolomic profiling identified 729 flavonoids, 308 of which were differentially accumulated metabolites (DAMs). Importantly, anthocyanin content increased upon ripening, while most other flavonoids decreased. Association analysis highlighted critical genes in anthocyanin biosynthesis, including upregulated *BZ1*, *AOMT*, 3MaT1, and *3MaT2*, which correlated with the accumulation of specific derivatives like cyanidin 3-O-(6-O27 malonyl)-β-D-glucoside and peonidin 3-glucoside, contributing to the hip's red color. Similarly, *CYP81E* genes were linked to isoflavonoid accumulation, while downregulated *CYP75B1* genes corresponded to decreased quercetin levels. These findings systematically elucidate the transcriptional and metabolic landscape of flavonoid biosynthesis during *R. rugosa* hip ripening, providing crucial insights for future genetic engineering aimed at enhancing flavonoid content and hip quality.

Citation: Li L, Jiang T, Guo S, Zhu H, Li W, et al. 2026. Integrated transcriptomic and metabolomic profiling elucidates the regulation of flavonoid composition and biosynthesis in *Rosa rugosa* hip. *Ornamental Plant Research* 6: e021 https://doi.org/10.48130/opr-0026-0014

Introduction

The wild *Rosa rugosa* is a shrub of the Rosaceae family. As a national second-class protected plant in China, it is an important germplasm resource for the cultivation of *R. rugosa* and the breeding of Rosaceae flowers[1]. The hip of *R. rugosa* has proven valuable in terms of food and medicine[2]. Patel studied phytonutrients and their physiological effects in *R. rugosa* hips, which contain vitamin C, proanthocyanidins, galactofat, and folate, as well as flavonoids, pectin, vitamin A, vitamin B complex, vitamin E, and minerals such as Ca, Mg, K, S, Si, Fe, Se, and Mn[3]. Due to the high nutritional value of *R. rugosa* hips, some countries and regions have incorporated them into their diets, consuming them as hips or fermenting them into wine, juice, and jam. Their hip extract has antioxidant, anti-inflammatory and immunomodulatory, anti-obesity and anti-diabetes, anti-cancer, and antibacterial effects[4,5]. Therefore, *R. rugosa* hips possess significant economic value, and efforts should be made to enhance hip quality for their application in fields such as food and medicine.

Flavonoids, which are widely present in various plants, play crucial roles in plant hormone signaling and stress responses, including protection against UV damage and defense against pathogen invasion. The basic structure of flavonoids consists of two benzene rings (A ring and B ring) connected by a three-carbon chain, forming a C6-C3-C6 skeleton structure. With the deepening understanding of flavonoids, more than 8,000 different types have been isolated and identified. The medicinal value of flavonoids continues to be uncovered, encompassing antioxidant, antibacterial, antiviral, and liver-protective properties, as well as their role in the treatment and prevention of cardiovascular and cerebrovascular diseases[6,7]. Anthocyanins, as an important subclass of flavonoids, are widely present in flowering plants[8]. They not only impart vibrant colors to petals, hips, and leaves but also serve as non-toxic antioxidants. Additionally, they exhibit functions such as inhibiting protein glycation and protecting vision, holding significant nutritional and health-promoting value[9]. Numerous studies have demonstrated the diversity in phytochemical composition among different *Rosa* species, as well as within accessions of the same species[10,11]. Flavonoids in *R. rugosa* hips have not yet been systematically studied in terms of their biosynthetic pathways.

To understand the accumulation patterns of flavonoids during the ripening process of *R. rugosa* hips, we measured the flavonoid content in both unripe and ripe hips. By integrating transcriptomic and metabolomic analyses, we identified flavonoid-associated metabolic pathways that change during hip ripening. This study provides a correlative basis for further exploration of potential molecular links underlying flavonoid accumulation and suggests candidate targets for future genetic engineering efforts aimed at modifying flavonoid content in *R. rugosa* hips.

Materials and methods

Plant samples and determination of chlorophyll, carotenoids, total flavonoids, and anthocyanin contents

The *R. rugosa* hips of different stages of development were harvested from the coast of Weihai, China (37°9'13.0'' N, 122°27'19.8'' E). Three wild *R. rugosa* populations were selected as biological replicates (n = 3). Within each population, fruit were collected from at least five individual plants and pooled together as one sample for subsequent measurements. Samples at different ripening stages were all collected from these three populations. After harvest, the seeds were quickly removed, and the remaining flesh was quickly frozen in liquid nitrogen and kept in a freezer at −80 °C. Based on previous studies on the classification of *R. rugosa* hip ripening stages[12], the *R. rugosa* hip was divided into three developmental stages according to morphological changes (Fig. 1). F0 hip is firm, shows no significant enlargement, and the hip color changes slightly from green, with no less than 10% of its surface turning yellow, pink, or red; the F1 hip is firm, its size is close to that of a mature hip, and the hip color turns orange or red; F2 the hip becomes soft and turns completely red.

The determination of chlorophyll, carotenoids, total anthocyanins, and total flavonoids was all carried out by spectrophotometry[13], whereas total flavonoids and anthocyanin content (mg/kg FW) were measured using Micro Plant Flavonoids Assay Kit (Solarbio, China, BC1335) and a plant anthocyanin test kit (Grace Biotechnology, China, G0126F), respectively. After 1 g of flesh was cut into small pieces and soaked in 95% ethanol in the dark for 24 h, the absorbance of the extract was measured at wavelengths 665, 649, and 470 nm. The calculation formulas for chlorophyll a, chlorophyll b, and carotenoids are as follows:

$$\mathrm{Ca\ (mg/L)} = 13.95 \times \mathrm{A665} - 6.88 \times \mathrm{A649}$$

$$\mathrm{Cb\ (mg/L)} = 24.96 \times \mathrm{A649} - 7.32 \times \mathrm{A665}$$

$$\mathrm{Ccar\ (mg/L)} = (1{,}000 \times \mathrm{A470} - 2.05 \times \mathrm{Ca} - 114.8 \times \mathrm{Cb})/245$$

RNA extraction and RNA-seq analysis

The RNAprep Pure Polysaccharide Polyphenol Plant Total RNA Extraction Kit (DP441, TIANGEN) was used to extract genomic RNA according to standard operating procedures provided by the manufacturer. mRNA with a polyA tail was enriched by Oligo (dT) magnetic beads. Then, the mRNA was used as a template to synthesize the first cDNA using reverse transcriptase and a random hexamer primer. The second strand cDNA was synthesized by DNA polymerase and then purified by DNA purification magnetic beads. The purified double-stranded cDNA was then end-repaired, a tail was added, and a sequencing joint was connected. Then, the fragment size was selected by using DNA purification magnetic beads, and the final cDNA library was obtained by PCR enrichment. Qualified libraries were sequenced by Illumina's NovaSeq 6000 platform, producing 150 bp paired-end reads for subsequent analysis. The genome sequence of *R. rugosa* (GCF_958449725.1) was downloaded from the NCBI website (www.ncbi.nlm.nih.gov/datasets/genome/GCF_958449725.1). The fastp v0.20.0 software was used for strict quality control of the data. Reads containing adapters were removed, and paired reads were discarded if the N content exceeded 10% or if the proportion of low-quality bases (Q ≤ 20) exceeded 50% in either read. Clean reads were compared with the reference genome using the HISAT2 v2.0.5 software. The Feature Counts v1.5.0 software was used to calculate the reads reading of each gene in each sample, and then the FPKM (Fragments Per Kilobase of transcript per Million fragments mapped) of each gene was calculated based on the length of the gene.

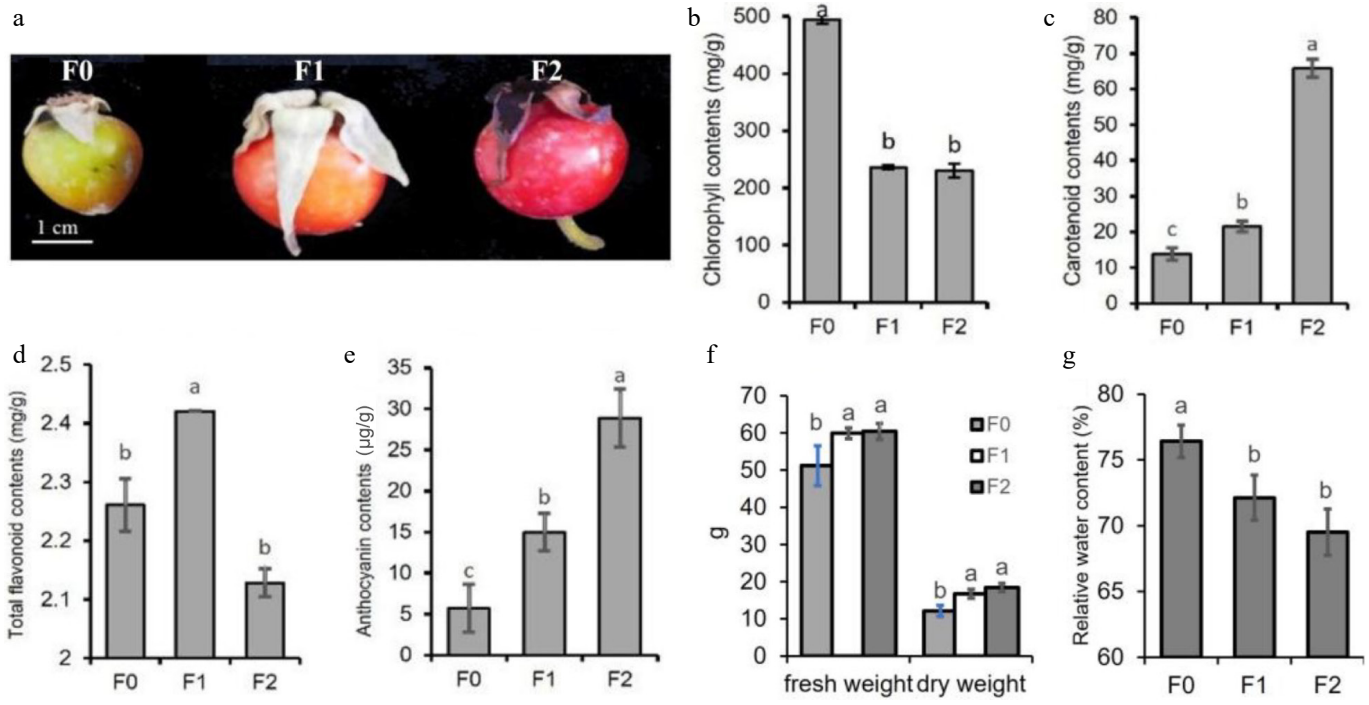

Fig. 1 The periods of hip harvest and the content of pigments in *R. rugosa* hips. (a) The periods of hip harvest. The period when the hip color changed from green to orange was identified as F0, the period when the hip turned into orange as F1, and the period when the hip turned red and softened as F2. (b) The content of chlorophyll. (c) The content of carotenoids. (d) The content of total flavonoids. (e) The content of anthocyanins. (f) The fresh and dry weight. (g) The relative water content.

Differential expression analysis was performed with DESeq2. The significance threshold was set at $|\log_2(\text{Fold Change})| \geq 1$ and false discovery rate (FDR) < 0.05, where the FDR was calculated using the Benjamini-Hochberg procedure. The identified DEGs were further subjected to GO enrichment analysis and KEGG pathway analysis.

Metabolomics analysis

The mature and immature hips were freeze-dried in a Scientz-100F for 63 h, and then ground to powder by a grinder (MM 400, Retsch). Then, 50 mg of the sample powder was weighed and 70% methanol-aqueous solution of 1,200 μL was added. The samples were swirled for 6 times for 30 s each time. The centrifuged supernatant was filtered by a microporous filter membrane (0.22 μm) for UPLC-MS/MS analysis.

The chromatographic column was an Agilent SB-C18 1.8 μm 2.1 mm × 100 mm. The mobile phase A is 0.1% formic acid aqueous solution. Mobile phase B is 0.1% acetonitrile solution. Elution gradient: 0~9 min, 5% B; 9~10 min, 95% B; 10~11 min, 5% B; 12~14 min, 5 B; the flow rate was 0.3 mL/min, the injection volume was 2 μL, and the column temperature was 40 °C.

The mass spectrum acquisition model uses information-dependent acquisition (IDA) to collect sample data. Ion spray voltage (IS): 5,000 V (positive ion mode)/−4,500 V (negative ion mode). The nebulizer gas (GS1), heating gas (GS2), and curtain gas (CUR) were 50, 60, and 25 psi, respectively. The ion collision energy (CE) is set to 10 eV.

The metabolites were quantified using multiple reaction monitoring (MRM). The 111 identified metabolites were subjected to an orthogonal partial least squares-discriminant analysis (OPLS-DA). The DAMs were screened based on the FC and VIP value of OPLS-DA. Metabolites with a VIP value ≥ 1 and FC ≥ 2 or FC ≤ 0.5 were considered DAMs. The DAMs were mapped to the KEGG pathway database for identification of a further 114 key pathways.

Integrated transcriptomic and metabolomic analysis

Pearson correlation coefficients were calculated for each gene–metabolite pair using the three biological replicates per time point as individual data points (i.e., $n = 3$ per correlation, no averaging). To control for multiple testing, the Benjamini–Hochberg false discovery rate (FDR) correction was applied to the correlation p-values. A pair was considered significantly correlated if it met both criteria: |Pearson's r| > 0.9 and FDR < 0.05.

To verify the reliability of annotations for key genes, homology analysis was performed. The protein sequences encoded by the candidate genes were aligned with functionally validated homologous sequences from model plants (*Arabidopsis thaliana*) and other species using BLAST software.

Statistical analyses

In this study, all experiments were performed with at least three biological replicates. SPSS 17.0 software (IBM, USA) was used to conduct one-way analysis and multiple comparison statistical analysis of the data ($p < 0.05$). The significance of differences was compared using Tukey's test.

Results

The contents of chlorophyll, carotenoids, total flavonoids, and anthocyanins in *R. rugosa* hips

The chlorophyll, carotenoids, total flavonoids, and anthocyanins content in *R. rugosa* hips at different developmental stages were detected. The chlorophyll content in *R. rugosa* hips at the F1 and F2 stages was significantly lower than that at F0, while the total flavonoid content was the highest at F1 (Fig. 1a, b, d). With hip ripening, the contents of anthocyanin and carotenoid gradually increased, which might be related to the change of hip peel color from green to red during the hip ripening process (Fig. 1c, e). Although the fresh weight significantly increased at stages F1 and F2 relative to stage F0, and dry weight and relative water content significantly decreased, no significant differences were observed in fresh weight, dry weight, or relative water content between F1 and F2 (Fig. 1f, g), suggesting that the changes in these parameters at F1 and F2 were not due to a water dilution effect.

Since the total flavonoid content peaked at the F1 stage, the F1–F2 period represents a critical ripening stage with active flavonoid metabolism (including anthocyanin synthesis), and the total flavonoid content at F0 was low; only the F1 and F2 stages were selected for subsequent transcriptomic and metabolomic sequencing.

Transcriptome analysis of the *R. rugosa* hip

To identify genes involved in *R. rugosa* hip ripening, RNA-seq analysis was performed using cDNA libraries extracted from F1 and F2 hips. A total of 370,096,556 clean reads were generated, and the data size of each sample is above 5.3 G. The Q20 bases of all samples were 97.96% and above, the Q30 bases were 93.73% and above, and the GC content is 48.91%~50.60%. The unique mapped reads were mapped to the reference sequences with match ratios ranging from 86.10% to 89.14%. These results indicated that the transcriptome sequencing was of high quality and could meet the requirements of follow-up experiments (Supplementary Table S1). PCA analysis indicated high correlation coefficients within the groups and considerable differences between the groups (Fig. 2a). The number of differentially expressed genes (DEGs) was 4,329, including 1,917 up and 2,415 downregulated DEGs (Fig. 2b). GO analysis was performed, and the DEGs were assigned to 33 biological process categories, 8 cellular components categories, and 10 molecular function categories (Fig. 2c). In the biological process, the 'secondary metabolic process' and 'photosynthesis' were the first two large subgroups.

To identify the potential biological pathway, DEGs were subjected to KEGG pathway enrichment analysis (Fig. 2d). Among the top 20 KEGG pathways, the 'Metabolic pathways' (ko01100), 'Biosynthesis of secondary metabolites' (ko01110), 'Photosynthesis' (ko00195), 'Photosynthesis - antenna proteins' (ko00196), and 'Plant hormone signal transduction' (ko04075) were the most significantly enriched pathways. These results suggest that the secondary metabolic processes are related to hip ripening.

Among upregulated DEGs, 62 DEGs were enriched into 'Biosynthesis of secondary metabolites', including 'isoflavonoid biosynthesis' (ko00943), 'anthocyanin biosynthesis' (ko00942), 'flavonoid biosynthesis' (ko00941), 'flavone and flavonol biosynthesis' (ko00944), etc (Fig. 2, Supplementary Table S2). Downregulated DEGs were mainly enriched in 'photosynthesis' (ko00195), 'Photosynthesis-antenna proteins' (ko00196), 'Metabolic pathways' (ko01100), 'Biosynthesis of secondary metabolites' (ko01110), and 'Glycolysis/Gluconeogenesis' (ko00010) (Fig. 2, Supplementary Table S3).

Through Weighted Gene Co-expression Network Analysis (WGCNA), the genes from six samples were ultimately clustered into 17 modules (Supplementary Fig. S1a). We focused on the turquoise module, which was significantly positively correlated with total flavonoid content (Supplementary Fig. S1b), and the blue module, which was significantly positively correlated with total anthocyanin content. The turquoise module contained 6,469 genes, and the blue

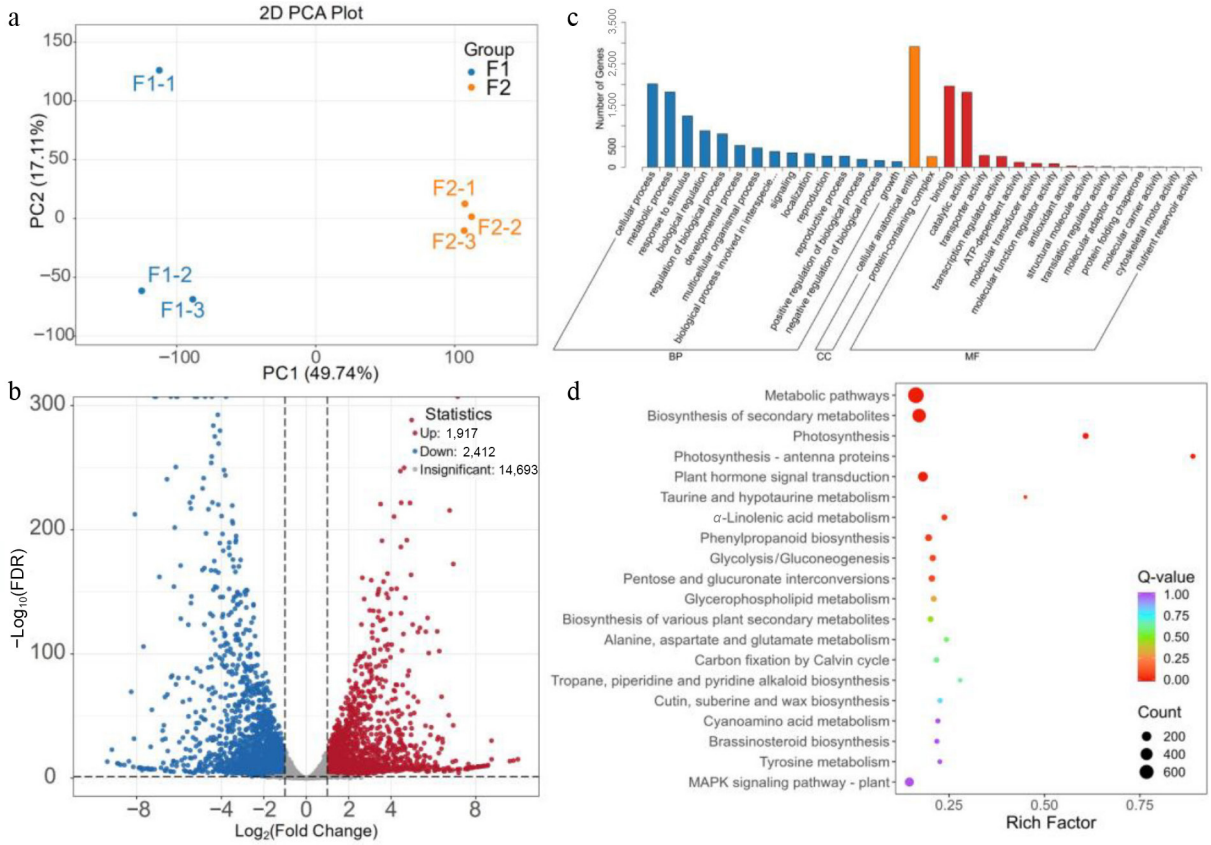

Fig. 2 Qualitative and quantitative analysis of the transcriptome data. (a) PCA analysis; (b) the volcano map of differentially expressed genes; (c) GO enrichment analysis; (d) KEGG enrichment analysis.

module contained 6,300 genes. Because the number of genes was too large to be displayed in a network diagram, we selected the MYB and bHLH transcription factors as well as proteins related to flavonoid biosynthesis, with a weight value greater than 0.67 for interaction shown in Supplementary Fig. S1b; similarly, MYB and bHLH transcription factors and proteins related to anthocyanin biosynthesis with a weight value greater than 0.67 were selected for interaction as shown in Supplementary Fig. S1c. Gene encoding anthocyanidin 3-O-glucoside-2″-O-glucosyltransferase (*C3GGT*, *LOC133729540*), a MYB transcription factor (*LOC133742674*), and two bHLH transcription factors (*LOC133708895* and *LOC133715311*) were hub genes in the turquoise module. Meanwhile, the hub genes in the blue module were MYB transcription factor (*LOC133715036*) and anthocyanidin 3-O-glucosyltransferase (*BZ1*, *LOC133713628*). These results indicate that MYB and bHLH transcription factors may play important roles in regulating the biosynthesis of flavonoids and anthocyanins.

Screening for DEGs of flavonoid biosynthesis pathway

Through in-depth mining of the transcriptome database of *R. rugosa* hip, a total of 38 DEGs were annotated on the flavonoid biosynthesis pathway by referring to the flavonoid biosynthesis pathway (ko00941) and reported flavonoid biosynthesis pathway (ko00942, ko00943, and ko00944) genes, of which 18 genes were upregulated, and 19 genes were downregulated in F2 hips (Supplementary Fig. S2).

A total of 328 transcription factors (TFs) were selected in differentially expressed genes (Supplementary Fig. S3), which were mainly distributed in 55 TF families, such as AP2/ERF (26), bHLH (25), MYB (21), C2H2 (21), WRKY (18), and C2C2 (15). It is well-established that the flavonoid biosynthesis enzymes are transcriptionally coordinated by the MYB-bHLH-WD40 (MBW) protein complex[13–15]. Hence, 21 MYB and 25 bHLH transcription factors could play important roles in the transcriptional regulation of enzyme genes in the flavonoid metabolism pathway.

Screening for differential metabolites in F1 and F2 hips

The difference of flavonoid metabolites in F1 and F2 hips was compared. A total of 729 metabolites were detected from six samples using UPLC-ESI-QTRAP-MS/MS and MRM. Principal component analysis (PCA) was performed on the data set using the three-dimensional scatter plot. Results showed the PC1, PC2, and PC3 accounted for 66.34%, 11.26%, and 8.48%, respectively. The extraction accumulation contribution rate of PC1, PC2, and PC3 was 86.08%. These two varieties were grouped separately, indicating significant differences in metabolism between the two samples and good identity between replicates (Fig. 3a).

The differential metabolites were divided into 12 categories, including 282 flavones, 256 flavonols, 94 tannins, 88 flavanones, 67 flavanols, 60 chalcones, 52 anthocyanins, 31 isoflavones, 20 proanthocyanidins, 15 flavanonols, eight aurones, and 44 other flavonoids (Fig. 3b–e). Substances with the highest content are flavonols, flavones, and dihydroflavones, and the substances with the lowest content are aurones, dihydroflavonols, and proanthocyanidins (Fig. 3f).

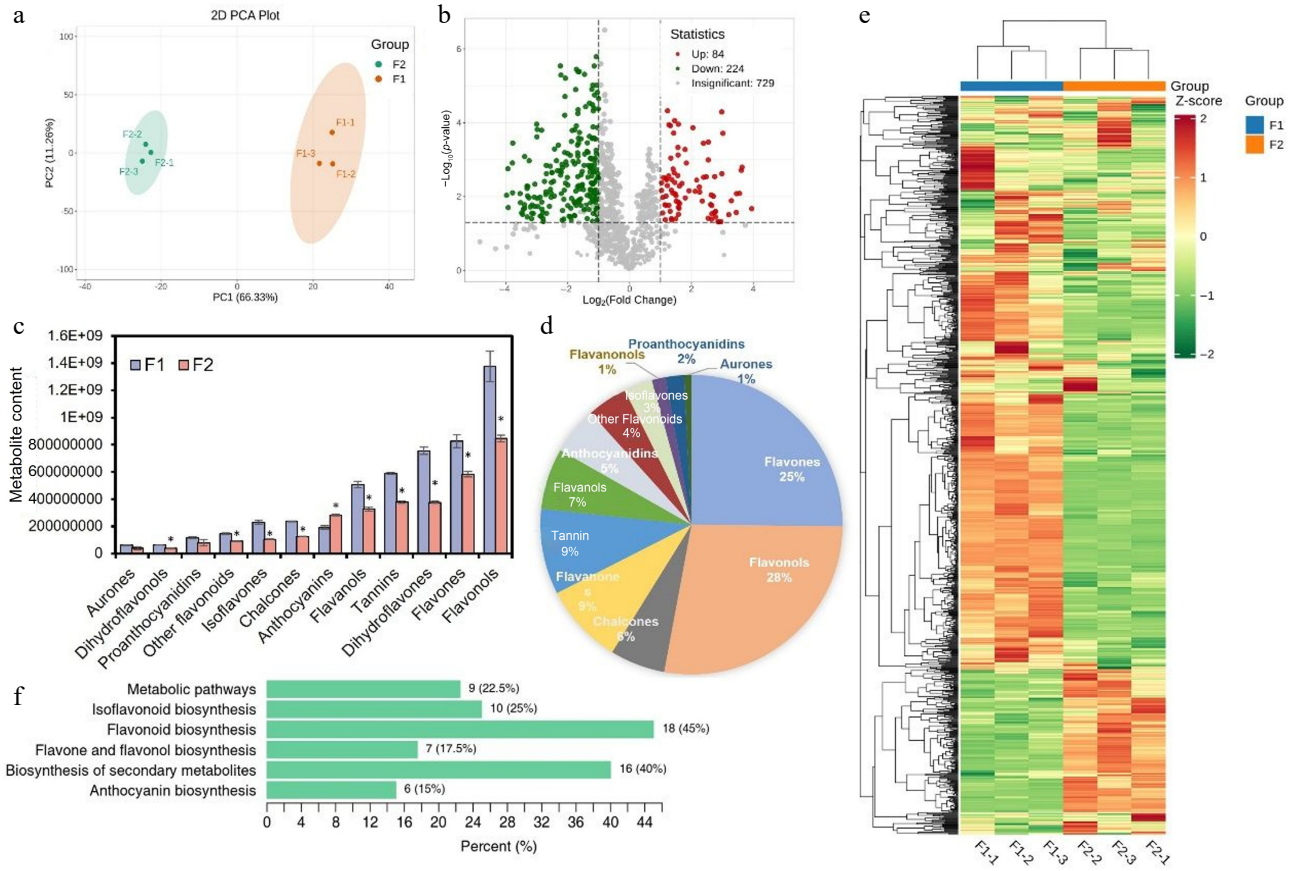

Fig. 3 Metabolome quality and differentially accumulated metabolites analysis. (a) PCA; (b) number of differential metabolites and up/downregulation; (c) changes in the content of various flavonoid components; (d) the proportion of various flavonoid components; (e) the heatmap of differential metabolites, with green representing downregulated metabolites, red representing upregulated metabolites; and (f) KEGG classification. The *x*-axis represents the proportion of each substance category. The *y*-axis represents the pathway. The numbers outside and inside the parentheses indicate the substance type and its percentage, respectively.

Association analysis of DEGs and DAMs in anthocyanin biosynthetic pathway

A total of 51 anthocyanins and their derivatives were detected, including 19 delphinidin derivatives and 26 cyanidin derivatives, while only 6 pelargonidin derivatives were detected, accounting for only 11.76% of the total. All the differential anthocyanin metabolites belonged to either cyanidin derivatives or delphinidin derivatives. These results suggest that the color of the F2 hip was mainly related to delphinidin and cyanidin derivatives.

During anthocyanin biosynthesis, the levels of five anthocyanin derivatives (malvidin 3-glucoside, petunidin 3-glucoside, delphinidin 3-O-3'',6''-O-dimalonylglucoside, cyanidin 3-O-(6-O-malonyl)-β-D glucoside, and peonidin 3-glucoside) were significantly increased, while the levels of 10 anthocyanin derivatives were decreased in the F2 hip. Among them, cyanidin 3-O-(6-O-malonyl)-β-D-glucoside and malvidin 3-glucoside were upregulated by more than 7-fold and 4-fold, respectively.

A pathway map containing metabolites and structural genes related to anthocyanin biosynthesis was constructed based on the enriched KEGG databases (Fig. 4). In the phenylalanine and flavonoid biosynthesis pathways, the expression of *DFR* (*LOC133713521*), two *CHS* (*LOC133718712* and *LOC133718713*), and *ANS* (*LOC133745281*) in the F2 hip was significantly higher than that in the control. In contrast, the expression of *4CH* (*LOC133708312*), *4CL* (*LOC133733552*), *CYP75B1* (*novel.1363*), and *ANR* (*LOC133729813*) was significantly downregulated in the F2 hip.

In the early stages of anthocyanin derivative synthesis, UDP-glucosyltransferase encoded by the BZ1 gene can convert anthocyanin aglycones into three anthocyanins (delphinidin 3-O-glucoside, cyanidin 3-O-glucoside, and pelargonidin 3-O-glucoside). Among the *BZ1* genes, two (*LOC133713628* and *LOC133710265*) were upregulated, while one (*LOC133738930*) was downregulated during hip ripening.

For the formation of anthocyanin derivatives, anthocyanin 3'-O-methyltransferase (AMOT) catalyzes 219 the methylation of the hydroxyl group of cyanidin 3-O-glucoside to produce peonidin 3-O-glucoside. Both the AMOT-encoding gene (*LOC133712310*) and peonidin 3-glucoside were upregulated in the F2 hip. Similarly, the genes encoding anthocyanin 3-O-glucoside-6''-O-malonyltransferase (*3MaT1*, *LOC133738337*) and anthocyanidin 3-O glucoside-3'',6''-O-dimalonyltransferase (*3MaT2*, *LOC133716052*) were upregulated in the F2 hip. In addition, 3MaT1 catalyzes the esterification of the 6-hydroxyl group of the glucose moiety in delphinidin/cyanidin 3-O-glucoside with malonic acid, forming delphinidin/cyanidin 3-O-(6-O-malonyl-β-D-glucoside). The content of cyanidin 3-O-(6-O-malonyl-β-D-glucoside) increased by 7.7-fold in the F2 hip. Additionally, 3MaT2 catalyzes the formation of delphinidin 3-O-(6′-O-malonyl)-β-D-glucoside, and the level of delphinidin 3-O-(6″-O-malonyl-β-D-glucoside)-3′-O-glucoside also increased by 2.56-fold. These results suggest that the AMOT, 3MaT1, and 3MaT2 encoding genes may play key roles in regulating anthocyanin synthesis.

In addition, several anthocyanin derivatives and their catalytic enzyme coding genes are downregulated, such as delphinidin/

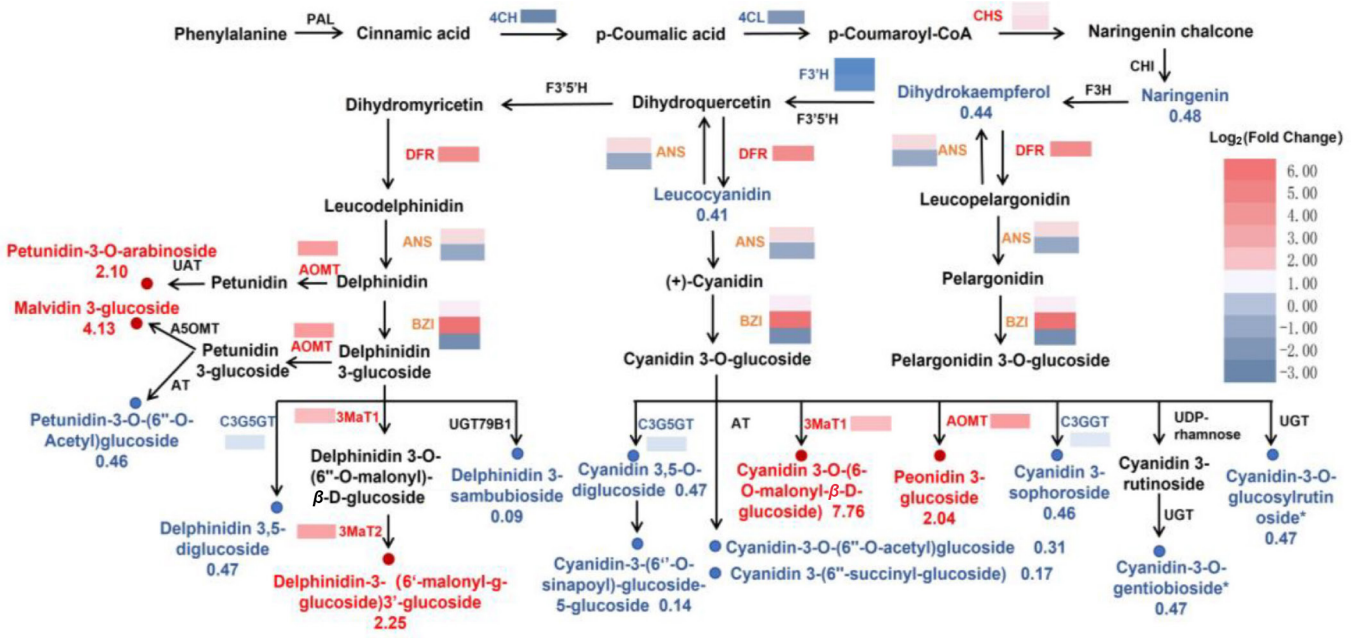

Fig. 4 Reconstruction of the anthocyanin biosynthetic pathway with differentially expressed enzyme genes (DEGs) and metabolites (DAMs) in F2 vs. F1.

Cyanidin 3,5-O-diglucoside and the *C3G5GT* gene, cyanidin 3-sophoroside and the *C3GGT* gene, indicating that the biosynthesis and accumulation of those anthocyanins above are significantly reduced in F2. This downregulation may be associated with the degradation or transformation of pigments, leading to changes in hip color, or it could reflect a shift in metabolic priorities towards other pathways, such as sugar accumulation or softening processes, which are critical for hip maturation and seed dispersal.

The heatmap of differential metabolites shows blue representing downregulated metabolites, red representing upregulated metabolites, and squares representing different transcripts of genes. In the heat maps, the blue-yellow-red scale represents low and high transcript expression, respectively. And red and blue fonts indicate significantly upregulated and downregulated metabolites, respectively. Chalcone synthase (CHS), chalcone isomerase (CHI), naringenin 3-dioxygenase (F3H), flavonoid 3'-monooxygenase (CYP75B1), anthocyanidin synthase (ANS), flavonoid 3',5'-hydroxylase (F3'5'H), flavonoid 3'-Hydroxylase (F3'H); bifunctional dihydroflavonol 4-reductase (DFR), anthocyanidin 3-O-glucosyltransferase (BZ1), anthocyanin 3'-O-methyltransferase (AOMT), anthocyanin 3',5'-O-methyltransferase (A5OMT), acyltransferase (AT), anthocyanidin 3-glucoside rhamnosyltransferase (UDP-rhamnose), anthocyanidin 3-O-glucoside-3'',6''-O-dimalonyltransferase (3MaT2), anthocyanin 3-O-glucoside-6''-O-malonyltransferase (3MaT1), anthocyanidin 3-O-glucoside-2''-O-glucosyltransferase (C3GGT), anthocyanidin 3-O glucoside 5-O-glucosyltransferase (C3G5GT).

Association analysis of DEGs and DAMs in the isoflavonoid, flavone, and flavonol biosynthetic pathways

In the isoflavonoid biosynthesis pathway, the levels of three DAMs (glycitein, genistin, and (–)-maackiain-3-O-glucosyl-6''-O-malonate) and three *CYP81E* genes were significantly upregulated (Fig. 5). Correlation network analysis showed that two CYP81E9 encoding genes (*LOC133724501* and *LOC133724502*) may be associated with the accumulation of glycitein, genistin, and (–)-maackiain-3-O-glucosyl-6''-O-malonate in F2 hips (Fig. 5). The downregulation of 3,9-dihydroxy pterocarpan, calycosin, and daidzin may be associated with the *CYP81E9* (*LOC133740171*) gene.

In the flavone and flavonol biosynthesis pathway, three DAMs (apiin, vitexin 2''-O-β-Dglucoside, and quercetin 3-sulfate) were increased, while four DAMs (quercetin, cosmetin, vitexin 2''-O-β-L-rhamnoside, and luteoloside) were decreased. *CYP75B1* genes encode flavonoid 3'monooxygenase (EC:1.14.14.82), which directly catalyzes the conversion of kaempferol to quercetin. The downregulated expression of the *CYP75B1* gene (*novel.1363*) may contribute to the decrease of quercetin accumulation in F2 hips.

Quercetin glycosides and kaempferol glycosides, as flavonol glycosides, affect color performance in plants mainly through copigmentation. For example, quercetin glycosides combine with cyanidin to make the red color more vivid. A total of four quercetin glycosides (quercetin 3-sulfate, quercetin 3-O-[6''-p-coumaroyl]-rutinoside, quercetin 3-O-[2''-O-rhamnosyl] galactoside, quercetin 3O-[6''-O-malonyl] glucosyl-5-O-glucoside) and one kaempferol glycoside (kaempferol-3-O-sulfonate) were increased in F2 hips, suggesting that those metabolites may also be involved in the orange color of *R. rugosa* hips.

The heatmap of differential metabolites shows blue representing downregulated metabolites, red representing upregulated metabolites, and squares representing different transcripts of genes. In the heat maps, the blue-yellow-red scale represents low and high transcript expression, respectively. And red and blue fonts indicate significantly upregulated and downregulated metabolites, respectively. Isoflavone/4'-methoxyisoflavone 2'-hydroxylase (CYP81E), Isoflavone 7-O-glucoside-6''-O-malonyltransferase (IF7MAT), Chalcone synthase (CHS), Flavonol synthase (FLS), Flavonoid 3'-hydroxylase (F3'H), Flavonol 3-sulfotransferase (F3ST), UDP-glycosyltransferase (UGT).

MYB and bHLH transcription factors are the master switches regulating the anthocyanin metabolic network, modulating the expression of anthocyanin synthesis genes by forming MYB-bHLH complexes or MYB-bHLH-WD40 complexes (MBW complexes)[14–17]. Thus, correlation tests were conducted to understand the relationship between metabolites and genes related to MYB and bHLH transcription factors, as well as flavonoid and anthocyanin biosynthesis.

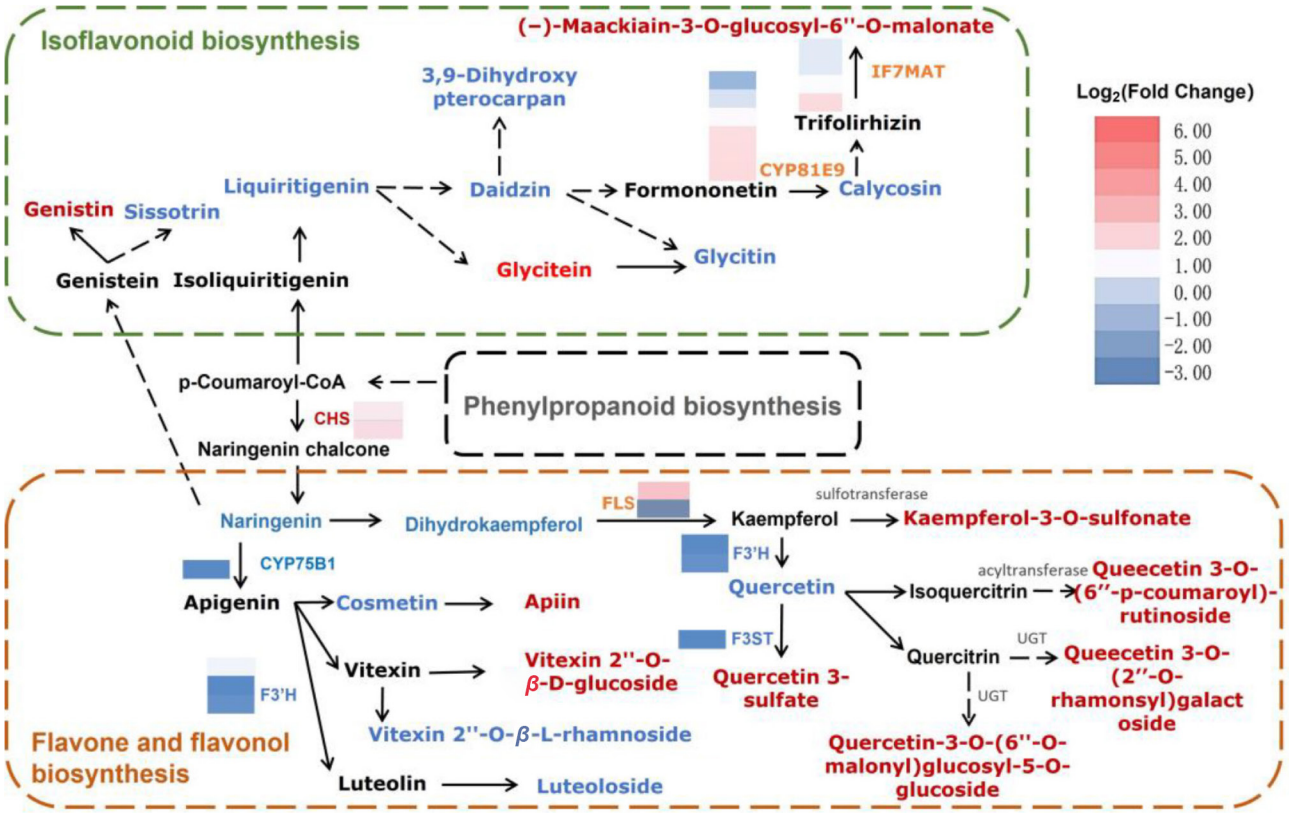

Fig. 5 Reconstruction of the flavone and flavonol biosynthetic pathway with differentially expressed enzyme genes (DEGs) and metabolites (DAMs) in F2 vs. F1.

The results with a Pearson correlation coefficient greater than 0.9 were selected. The key gene functional annotation and differential expression statistics were displayed in Supplementary Table S4. The result exhibited that 27 differentially expressed structural genes related to flavonoid and anthocyanin biosynthesis were co-expressed with 15 anthocyanin-related metabolites and 15 TFs (Fig. 6). Among the 27 DEGs, *LOC133713628 (BZ1)* was positively correlated with the two Delphinidin derivatives (Malvidin 3-glucoside [Zbhp002708] and Delphinidin 3-O-3'',6''-O-dimalonylglucoside [pmb0558]). Two CYP81B encoding genes *LOC133724501*, and *LOC133724502*, were positively correlated with three Isoflavonoids (genistin, glycitein, and (−)-Maackiain-3-O-glucosyl-6''-O-malonate). Regarding flavone and flavonol biosynthesis, *LOC133727523* (*PG3*) was positively correlated with the levels of Quercetin 3-sulfate (Lmfn005487) and Apigenin 7-O-(*β*-D-apiosyl-[1->2]-*β*-D-glucoside)*, (pmf0472), and negatively correlated with Quercetin (MWSHY0029).

Discussion

The *R. rugosa* hip, displaying vibrant red-orange hues, ripens by late summer and can persist on the plant for several months even after the foliage withers in autumn and winter, offering significant ornamental value. Studies have shown that there are significant differences in the flavonoid content in the hips of *Rosa* plants at different maturity levels[10,18].

Transformation of key flavonoids during hip ripening

The ripening process is a critical window for flavonoid transformation. Although the contents of total flavonoids decreased during the ripening process, 308 metabolites underwent significant changes in mature *R. rugosa* hips, with 93 flavones and 71 flavonols showing substantial content differences. From the F1 period on, the chlorophyll content decreased significantly in *R. rugosa* hips (Fig. 2a). Transcriptome analysis also revealed the downregulation of photosynthesis-related genes and the upregulation of secondary metabolism-related genes (particularly flavonoid synthesis) during hip ripening. This indicates that chloroplasts degrade during ripening, and photosynthesis gives way to the synthesis and accumulation of substances responsible for color, aroma, and taste. The downregulation of photosynthesis likely reallocates resources and energy (such as carbon skeletons and ATP) to secondary metabolic pathways, supporting the biosynthesis of pigments and flavor compounds like anthocyanins and flavonoids.

Multiple components with well-defined bioactivities, such as isoflavones and quercetin derivatives, were specifically upregulated in mature hips. Isoflavones (e.g., genistin, glycitein) are renowned as phytoestrogens and have demonstrated potential in epidemiological and clinical studies for preventing breast and prostate cancers, improving menopausal syndrome, and promoting cardiovascular health[19]. In mature hips, seven isoflavones (7-hydroxy-3'-methoxy-isoflavone-7-primeveroside, hlycitein, astrapterocarpan 3-O-malonyl glucoside, [–]-maackiain-3-O-glucosyl-6''-O-malonate, genistin, genistein-8-C-glucoside-O apiosyl, and calycosin-7-O-glucoside) accumulated significantly, suggesting that *R. rugosa* hip is a potential natural source of isoflavones. Although the content of free quercetin (quercetin aglycone) decreased, the levels of its various glycosidic forms (e.g., quercetin 3-sulfate) increased. Quercetin is a recognized potent antioxidant and anti-inflammatory agent. Its glycosidic forms exhibit increased water solubility and enhanced metabolic stability, generally leading to higher bioavailability[20,21].

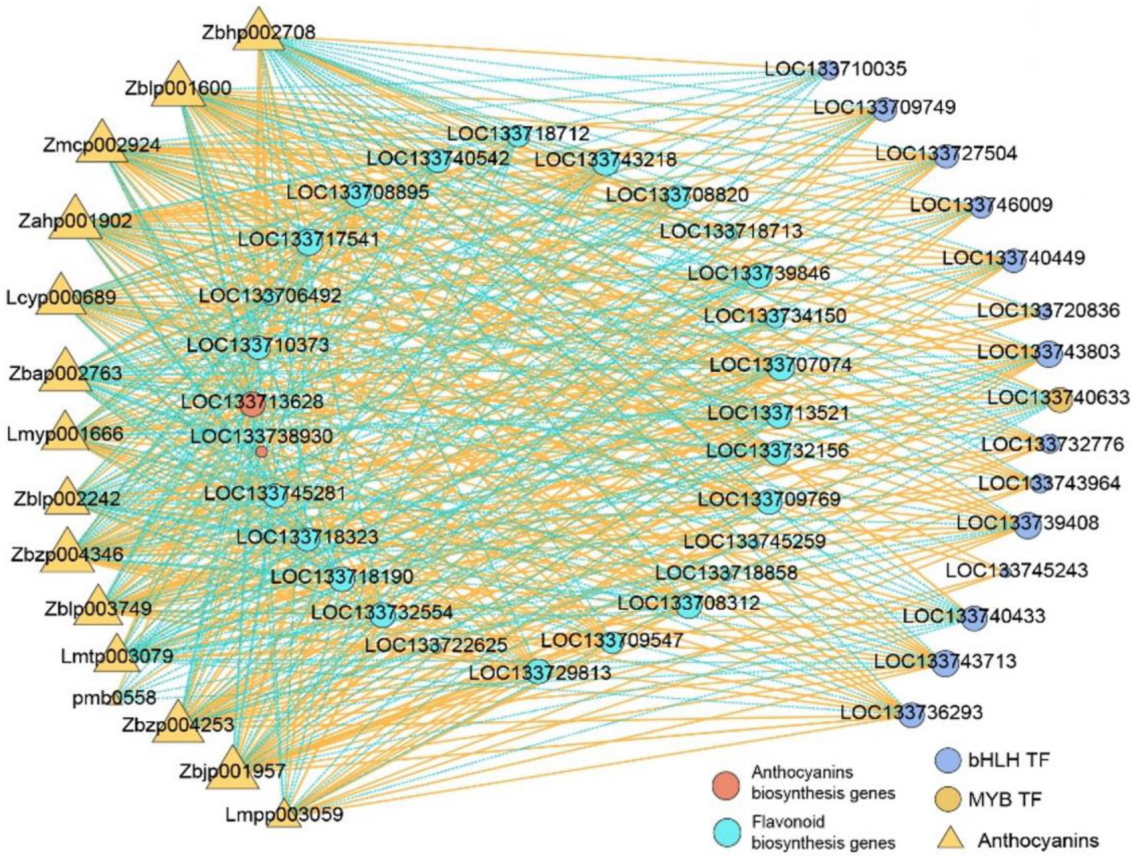

Fig. 6 The co-expression analysis of MYB and bHLH TFs (|Fold change | ≥ 4), DEGs, and DAMs involved in anthocyanin biosynthesis in F2 vs. F1. *R* was more than 0.9 and less than −0.9, with $p < 0.05$.

The accumulation of these substances implies that mature *R. rugosa* hips possess stronger free radical scavenging ability and anti-inflammatory potential. Proanthocyanidins and tannins are renowned for their powerful antioxidant, antimicrobial, and protective effects on cardiovascular and urinary tract health[22,23]. Ninety-four tannins and twenty proanthocyanidins were detected in *R. rugosa* hips. These results indicate that *R. rugosa* hips are rich in a variety of flavonoid compounds with proven health-promoting functions, forming a solid material basis for their use as a functional food or natural medicinal resource. The maturity of the *R. rugosa* hip directly determines the composition and content of its flavonoids, thereby defining its nutritional and medicinal value. Therefore, selecting the appropriate harvest time is crucial for maximizing the health benefits of *R. rugosa* hips.

Regulation of hip pigment changes and anthocyanin synthesis

The rich carotenoids and anthocyanins in the hips are the primary pigments responsible for plant coloration. However, research on the pigment composition and regulatory mechanisms in wild *R. rugosa* hips remains unclear. Our studies showed that as the hip continues to ripen, the contents of carotenoids and anthocyanins both increase significantly, and the content of these pigments varies, leading to distinct color differences. The red of mature hips (F2) was primarily determined by cyanidin and delphinidin derivatives, with pelargonidin derivatives accounting for a very small proportion. Concurrently, several key structural genes (e.g., *CHS*, *DFR*, *ANS*, *BZ1*) in the early stages of anthocyanin synthesis were coordinately upregulated, indicating the specific activation of the cyanidin and delphinidin pathways. Furthermore, the upregulation of late modification genes for anthocyanin glycosides (e.g., *AOMT*, *3MaT1*, *3MaT2*) led to a sharp increase in specific derivatives (e.g., malonylcyanidin glucoside). The AOMT gene can methylate cyanidin glucoside, which not only increases the water solubility and stability of anthocyanins but also causes a spectral red shift, crucial for forming specific orange/red hues. Research found that grapevine AOMT catalyzes both 3' and 5' O-methylation of anthocyanins[24]. In grape, the AOMT2 gene mutation significantly affected the enzyme-specific catalytic efficiency for the 3'-O-methylation of delphinidin 3-glucoside[25]. During *R. rugosa* hip ripening, the *AOMT* gene was upregulated 7.7-fold. The *3MaT1* and *3MaT2* genes can malonylate delphinidin/cyanidin 3-O-glucoside, producing various delphinidin/peonidin derivatives, further enriching the diversity of hip color[26,27].

Multi-omics association reveals the regulatory network of flavonoid biosynthesis in *R. rugosa* hips and identifies key targets

Integrated multi-omics analysis revealed a high consistency between gene expression patterns and metabolite accumulation levels. For instance, there was a strong positive correlation between the *BZ1* gene and specific delphinidin derivatives, and between *CYP81E* genes and isoflavone metabolites (e.g., genistin). The down-regulation of the *CYP75B1* gene was associated with a decrease in quercetin content. This provides strong, direct evidence for hypothesizing the 'gene-enzyme-metabolite' regulatory pathway of flavonoid biosynthesis in *R. rugosa* hip and offers potential molecular targets for future directed enhancement of these specific active components through biotechnology or cultivation practices.

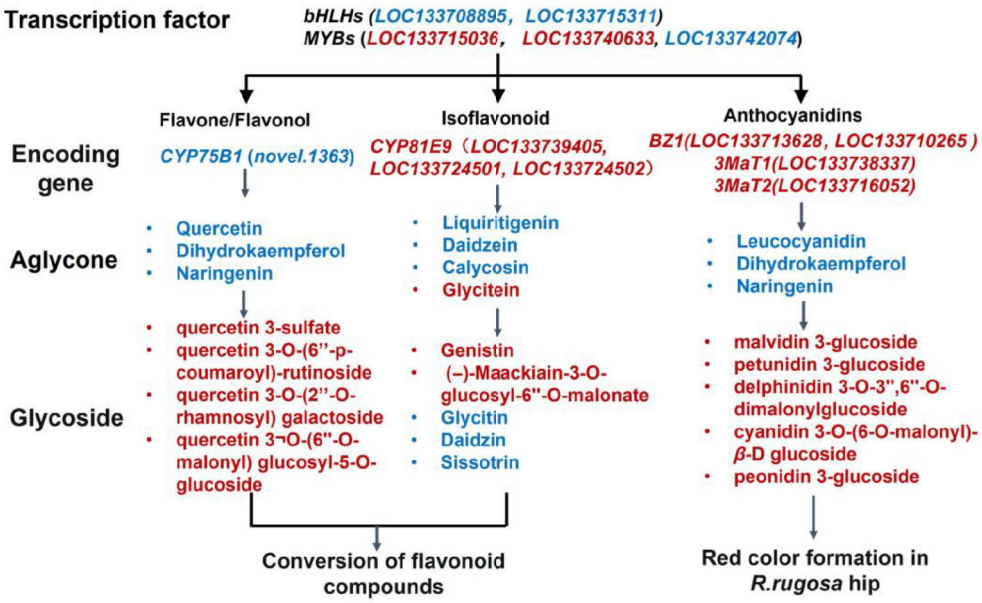

Fig. 7 Core regulatory model diagram of flavonoid metabolism during *R. rugosa* hip ripening. Red and blue roman font indicates significantly upregulated and downregulated metabolites, respectively. Red and blue italic font indicates significantly upregulated and downregulated genes, respectively.

MYB genes, involved in regulating flavonoid biosynthesis, thereby influencing flower organ or hip coloration, have been isolated from various plants such as petunia[28], gerbera[29], tomato[30], grape[31], apple[32], and gentian[33]. For example, Schwinn et al. isolated three R2R3 MYB transcription factors from snapdragon petals and found they influence pigment accumulation by activating the expression of different key enzyme genes in the anthocyanin synthesis pathway[34]. Similarly, bHLH transcription factors regulating anthocyanin synthesis-related genes have been cloned and functionally characterized in many plants, such as *Arabidopsis* TT2[35] and petunia (AN1, AN4, AN11)[36]. A total of 1 MYB and 14 bHLH transcription factors were identified among the DEGs, and the co-expression network analysis supported the regulatory function of MYB and bHLH in the flavonoid biosynthesis pathway (Supplementary Fig. S1, Fig. 6). Future regulation of these key transcription factors could potentially enable the overall improvement of the nutritional quality of *R. rugosa* hips.

Conclusions

This study demonstrates that *R. rugosa* hips undergo a profound metabolic reprogramming of flavonoids during ripening. This not only shapes their external color but also constructs their nutritional and medicinal foundation as a high-value functional food. We have not only identified the accumulation patterns of a series of flavonoids, such as isoflavones and flavonol glycosides, closely related to health benefits, but also preliminarily deciphered the underlying key structural genes and transcription factors (Fig. 7). In ripe hips, although the content of most anthocyanins, isoflavones, flavones, and flavonol aglycones significantly decreases or show no significant change, the contents of several derivatives are significantly upregulated. The increased levels of anthocyanin derivatives such as malvidin 3-glucoside, petunidin 3-glucoside, delphinidin 3-O-3'',6''-O-dimalonylglucoside, cyanidin 3-O-(6-O-malonyl)-β-D-glucoside, and peonidin 3-glucoside may account for the rise in total anthocyanin content and the red coloration of ripe hips. Furthermore, the results of co-expression network analysis supported that several MYB and bHLH transcription factors may be involved in regulating the transition of flavonoid compounds during fruit ripening. This provides a theoretical basis for molecular marker-assisted selection and molecular breeding to develop *R. rugosa* varieties with higher flavonoid nutrient content.

Author contributions

The authors confirm their contributions to the paper as follows: study conception and design: Li L, Jiang T; data collection: Zhang C, Guo S, Lu Y; analysis and interpretation of results: Zhu H, Li W; draft manuscript preparation: Li L, Zhang C, Jiang T; funding acquisition and resources: Zhang C, Lu Y. All authors reviewed the results and approved the final version of the manuscript.

Data availability

The datasets generated during and/or analyzed during the current study are available from the corresponding author upon reasonable request.

Acknowledgments

This research was supported by the Key R&D Program of Shandong Province 'Accurate Identification and Innovative Utilization of Forest and Grass Germplasm Resources', China (2024LZGC003), the Young Scientists Fund of the National Natural Science Foundation of China (32201611), and the Key R&D Program of Shandong Province, China (2025CXPT149).

Conflict of interest

The authors declare that they have no conflict of interest.

Supplementary information accompanies this paper online at: https://doi.org/10.48130/opr-0026-0014.

Dates

Received 29 December 2025; Revised 29 April 2026; Accepted 14 May 2026; Published online 4 June 2026

References

[1] Yang ZY, Zhao LY, Xu ZD. 2010. 野生玫瑰与栽培玫瑰对盐胁迫反应的比较研究 [Comparison of the resistance to salt stress between wild plants and cultivars of *Rosa rugosa*]. *山东林业科技 [Shandong Forestry Science and Technology]* 40:43−44,50 (in Chinese)

[2] Chen F, Su L, Hu S, Xue JY, Liu H, et al. 2021. A chromosome-level genome assembly of rugged rose (*Rosa rugosa*) provides insights into its evolution, ecology, and floral characteristics. *Horticulture Research* 8:141

[3] Patel S. 2017. Rose hip as an underutilized functional food: evidence-based review. *Trends in Food Science & Technology* 63:29−38

[4] Cendrowski A, Kraśniewska K, Przybył JL, Zielińska A, Kalisz S. 2020. Antibacterial and antioxidant activity of extracts from rose fruits (*Rosa rugosa*). *Molecules* 25:1365

[5] Çolak AM , Alan F. 2025. Determination of pomological and chemical properties of some rosehip (*Rosa* spp.) genotypes growing naturally in Kayseri province. *ISPEC Journal of Agricultural Sciences* 9:621−629

[6] Duarte M, Santos Pedrosa S, Khusial PR, Madureira AR. 2025. The biological potential and health-benefits of flavonoids: a review and development opportunities. *Chemico-Biological Interactions* 421:111755

[7] Peluso I, Miglio C, Morabito G, Ioannone F, Serafini M. 2015. Flavonoids and immune function in human: a systematic review. *Critical Reviews in Food Science and Nutrition* 55:383−395

[8] Sarma AD, Sreelakshmi Y, Sharma R. 1997. Antioxidant ability of anthocyanins against ascorbic acid oxidation. *Phytochemistry* 45:671−674

[9] Yao LH, Jiang YM, Shi J, Tomás-Barberán FA, Datta N, et al. 2004. Flavonoids in food and their health benefits. *Plant Foods for Human Nutrition* 59:113−122

[10] Dolek U, Gunes M, Genc N, Elmastas M. 2018. Total phenolic compound and antioxidant activity changes in rosehip (*Rosa* sp.) during ripening. *Journal of Agricultural Science and Technology* 20:817−828

[11] Andersson SC, Rumpunen K, Johansson E, Olsson ME. 2011. Carotenoid content and composition in rose hips (*Rosa* spp.) during ripening, determination of suitable maturity marker and implications for health promoting food products. *Food Chemistry* 128:689−696

[12] Medveckienė B, Levickienė D, Vaitkevičienė N, Vaštakaitė-Kairienė V, Kulaitienė J. 2023. Changes in pomological and physical parameters in rosehips during ripening. *Plants* 12:1314

[13] Arora N, Lo E, Philippidis GP. 2022. A two-prong mutagenesis and adaptive evolution strategy to enhance the temperature tolerance and productivity of *Nannochloropsis oculata*. *Bioresource Technology* 364:128101

[14] Appelhagen I, Lu GH, Huep G, Schmelzer E, Weisshaar B, et al. 2011. TRANSPARENT TESTA1 interacts with R2R3-MYB factors and affects early and late steps of flavonoid biosynthesis in the endothelium of *Arabidopsis thaliana* seeds. *The Plant Journal* 67:406−419

[15] Liu S, Zhang H, Meng Z, Jia Z, Fu F, et al. 2025. The *LncNAT11*–MYB11–F3'H/FLS module mediates flavonol biosynthesis to regulate salt stress tolerance in *Ginkgo biloba*. *Journal of Experimental Botany* 76:1179−1201

[16] Feller A, Machemer K, Braun EL, Grotewold E. 2011. Evolutionary and comparative analysis of MYB and bHLH plant transcription factors. *The Plant Journal* 66:94−116

[17] Shi Y , Lu T , Lai S, Li S, Zhang L, et al. 2024. *Rosa rugosa* R2R3-MYB transcription factors RrMYB12 and RrMYB111 regulate the accumulation of flavonols and anthocyanins. *Frontiers in Plant Science* 15:1477278

[18] Chen NF, Zhang L. 2005. 金樱子黄酮类化合物的初步研究 [Preliminary study on flavonoid compounds from *Rosa laevigata* Michx]. *中国林副特产 [Forest By-Product and Speciality in China]* 2005:2−4 (in Chinese)

[19] Wiseman H, O'Reilly JD, Adlercreutz H, Mallet AI, Bowey EA, et al. 2000. Isoflavone phytoestrogens consumed in soy decrease F_2-isoprostane concentrations and increase resistance of low-density lipoprotein to oxidation in humans. *The American Journal of Clinical Nutrition* 72:395−400

[20] Erlund I, Kosonen T, Alfthan G, Mäenpää J, Perttunen K, et al. 2000. Pharmacokinetics of quercetin from quercetin aglycone and rutin in healthy volunteers. *European Journal of Clinical Pharmacology* 56:545−553

[21] Vyniarska AV. 2024. Quercetin: biological activity, therapeutic potential and prospects of the use. *Scientific Messenger of LNU of Veterinary Medicine and Biotechnologies* 26:242−247

[22] Adhimi CS, Sakti AS, Pratiwi ED, Khan MA. 2024. Article review: in vitro, in vivo, and clinical trial data on proanthocyanidin compounds. *Surya* 16:63−71

[23] Liu C, Bolling BW. 2024. Dietary proanthocyanidins for improving gut immune health. *Current Opinion in Food Science* 56:101133

[24] Lücker J, Martens S, Lund ST. 2010. Characterization of a *Vitis vinifera* cv. Cabernet Sauvignon 3', 5'-*O*-methyltransferase showing strong preference for anthocyanins and glycosylated flavonols. *Phytochemistry* 71:1474−1484

[25] Fournier-Level A, Hugueney P, Verriès C, This P, Ageorges A. 2011. Genetic mechanisms underlying the methylation level of anthocyanins in grape (*Vitis vinifera* L.). *BMC Plant Biology* 11:179

[26] D'Auria JC, Reichelt M, Luck K, Svatoš A, Gershenzon J. 2007. Identification and characterization of the BAHD acyltransferase malonyl CoA: anthocyanidin 5-*O*-glucoside-6''-*O*-malonyltransferase (At5MAT) in *Arabidopsis thaliana*. *FEBS Letters* 581:872−878

[27] Suzuki H, Nakayama T, Nishino T. 2003. Proposed mechanism and functional amino acid residues of malonyl-CoA: anthocyanin 5-*O*-glucoside-6'''-*O*-malonyltransferase from flowers of *Salvia splendens*, a member of the versatile plant acyltransferase family. *Biochemistry* 42:1764−1771

[28] Quattrocchio F, Verweij W, Kroon A, Spelt C, Mol J, et al. 2006. PH4 of Petunia is an R2R3 MYB protein that activates vacuolar acidification through interactions with basic-helix-loop-helix transcription factors of the anthocyanin pathway. *The Plant Cell* 18:1274−1291

[29] Elomaa P, Uimari A, Mehto M, Albert VA, Laitinen RAE, et al. 2003. Activation of anthocyanin biosynthesis in *Gerbera hybrida* (Asteraceae) suggests conserved protein-protein and protein promoter interactions between the anciently diverged monocots and eudicots. *Plant Physiology* 133:1831−1842

[30] Mathews H, Clendennen SK, Caldwell CG, Liu XL, Connors K, et al. 2003. Activation tagging in tomato identifies a transcriptional regulator of anthocyanin biosynthesis, modification, and transport. *The Plant Cell* 15:1689−1703

[31] Kobayashi S, Goto-Yamamoto N, Hirochika H. 2004. Retrotransposon-induced mutations in grape skin color. *Science* 304:982

[32] Espley RV, Hellens RP, Putterill J, Stevenson DE, Kutty-Amma S, et al. 2007. Red colouration in apple fruit is due to the activity of the MYB transcription factor, MdMYB10. *The Plant Journal* 49:414−427

[33] Nakatsuka T, Haruta KS, Pitaksutheepong C, Abe Y, Kakizaki Y, et al. 2008. Identification and characterization of R2R3-MYB and bHLH transcription factors regulating anthocyanin biosynthesis in gentian flowers. *Plant and Cell Physiology* 49:1818−1829

[34] Schwinn K, Venail J, Shang Y, Mackay S, Alm V, et al. 2006. A small family of *MYB*-regulatory genes controls floral pigmentation intensity and patterning in the genus *Antirrhinum*. *The Plant Cell* 18:831−851

[35] Nesi N, Jond C, Debeaujon I, Caboche M, Lepiniec L. 2001. The Arabidopsis *TT2* gene encodes an R2R3 MYB domain protein that acts as a key determinant for proanthocyanidin accumulation in developing seed. *The Plant Cell* 13:2099−2114

[36] Spelt C, Quattrocchio F, Mol JNM, Koes R. 2000. *Anthocyanin1* of petunia encodes a basic helix-loop-helix protein that directly activates transcription of structural anthocyanin genes. *The Plant Cell* 12:1619−1631